

DAM SAFETYModelling turbulent Seepage in Rock-fill Dams

Rapport 06:70

Modelling turbulent Seepage in Rock-fill Dams

Elforsk rapport 06:70

Per Sundqvist, James Yang Vattenfall Research & Development AB

Förord

Stockholm november 2006

Denna rapport är ett delresultat inom Elforsk ramprogram Dammsäkerhet.

Kraftindustrin har traditionellt satsat avsevärda resurser på forsknings och utvecklingsfrågor inom dammsäkerhetsområdet, vilket har varit en förutsättning för den framgångsrika utvecklingen av vattenkraften som energikälla i Sverige.

Målen för programmet är att långsiktigt stödja branschens policy, dvs att:

- Sannolikheten för dammbrott där människoliv kan vara hotade skall hållas på en så låg nivå att detta hot såvitt möjligt elimineras.
- Konsekvenserna i händelse av dammbrott skall genom god planering såvitt möjligt reduceras.
- Dammsäkerheten skall hållas på en god internationell nivå.

Prioriterade områden är Teknisk säkerhet, Operativ säkerhet och beredskap samt Riskanalys.

Ramprogrammet har en styrgrupp bestående av: Jonas Birkedahl – FORTUM, Malte Cederström - Vattenfall Vattenkraft, Anders Isander – E.ON, Lennart Markland – Vattenregleringsföretagen, Urban Norstedt - Vattenfall Vattenkraft, Gunnar Sjödin – Vattenregleringsföretagen, Olle Mill Svenska Kraftnät samt Lars Hammar - Elforsk

Lars Hammar Elforsk AB

Summary

Turbulent seepage in porous media represents a classical topic. An analytical solution in two dimensions for turbulent seeping flow in homogenous and isotropic rock-fill dams is revisited and its derivation is simplified. Its usefulness is improved in a sense that explicit expressions of the seepage point location in the downstream slope and the phreatic surface are worked out. The seeping discharge can be easily computed, although its accuracy relies on a good knowledge of the turbulent permeability. Laboratory experiments of turbulent seepage in a 1.9 m high rock-fill dam were previously made in a flume at Vattenfall R&D, Älvkarleby. CFD computations in 2D are also performed with the commercial code FLUENT, where the dam in question is modelled as a porous medium and the phreatic surface is determined with a two-phase (water-air) model. Results from the analytical solution and CFD computations are compared with the experimental data, indicating that the agreement is generally good. CFD modelling gives the best correspondence to the experiments. The analytical approach is useful when an approximate answer is needed quickly.

Content

1	BACKGROUND	7
2	ANALYTICAL SOLUTIONS	8
	2.1 PHREATIC SURFACE AND SEEPAGE DISCHARGE	9
_	2.2 SEEPAGE POINT LOCATION	
3	EXPERIMENTS	14
4	NUMERICAL SOLUTIONS, CFD	15
5	RESULTS AND COMPARISONS	18
	5.1 SEEPAGE POINT LOCATION	18
	5.2 SEEPAGE DISCHARGE	19
	5.3 PHREATIC SURFACE	19
6	CONCLUSIONS	22

1 Background

Many embankment dams in Scandinavia were constructed 30 - 60 years ago. Due to the updated design flood and safety guidelines as well as aging, safety evaluation and rebuilding constitute an important part of the ongoing efforts by the hydropower sector to raise the safety level of these dams. Field investigations, as well as laboratory studies, have been made, with the purpose of understanding the seepage behaviors in embankment dams.

With this in the background, a joint project was carried out in Norway during 2001 - 03. The test site is located on the Røssåga river, close to the town Mo i Rana. The embankment dams are constructed with various materials of rock-fill, gravel and clay. Some are of homogeneous type, while the others have central moraine core. Tests of seepage characteristics, stability and dam break mechanism were performed for a number of 6 m high and 36 m long embankment dams. Most of the dams are brought to complete failure, but tests are conducted in stages to gather such data as material properties, allowed seepage capacity and so on.

In connection to the project, there has been a renewed interest in analytical solutions of the turbulent seepage through rock-fill dams. Results of seepage modelling are often used in the slope stability analysis of embankment dams. An analytical solution was developed by Solvik (1966). His result has, however, been questioned as its agreement with the experimental data proves to be poor.

In this report, we revisit Solvik's formulae and eliminate the error due to ambiguity in parameter definition or misprints. Furthermore, an approximate expression developed by Solvik for the solution of seepage point location in the downstream slope is replaced by an analytical formula. The analytical expression for the phreatic surface through the dam is made more explicit. The new expressions are compared with the measurements from laboratory experiments and 2D numerical flow computations.

The report is organized as follows. Section 2 contains the derivation of analytical solutions for the phreatic surface, seepage discharge and seepage point location. Section 3 consists of a brief description of the experimental cases that are used for comparisons. Section 4 describes the 2D CFD computations using the computer code FLUENT. The results are compared with each other in Section 5. Section 6 contains concluding remarks.

2 Analytical solutions

The geometry of the embankment dam for deriving analytical solutions of turbulent seeping flow is denoted in **Figure 2.1**. Considering a homogenous isotropic embankment dam resting on a horizontal foundation. The downstream slope is vertical/horizontal = 1/n. The up- and downstream water depths above the foundation are denoted as H and h (m), respectively. The flow is assumed to be directed mainly along the negative x-axis. The seeping discharge, q, is given in (m³/s)/m, i.e. discharge per meter along the dam. The intersection point of the reservoir water stage with the upstream slope and the seeping outflow point in the downstream slope are denoted as (L, H) and (x₀, y₀), respectively

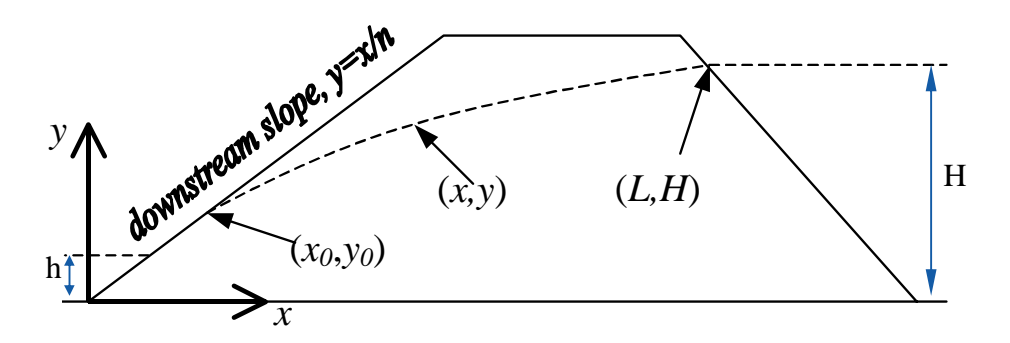


Figure 2.1: Geometry of the dam and notation.

Solvik (1966) treats the problem by assuming a horizontal flow with a velocity profile constant in the y-direction. The two relations that are used as starting points for his derivation are

$$q = Vy \tag{1}$$

and

$$V^2 = k_{t}I. (2)$$

Equation (1) says that the unit discharge q is the product of the velocity and the height of the phreatic surface. Equation (2) is the relation between the hydraulic gradient, I=dy/dx, and the velocity, V (m/s), in turbulent flow through porous media. The constant k_t is the turbulent permeability.

2.1 Phreatic surface and seepage discharge

Combining equations (1) and (2) and eliminating the velocity V yields an ordinary differential equation in y(x)

$$y^2 y' = q^2 / k_t, \quad x_0 < x < L,$$
 (3)

with the general solution

$$\frac{1}{3}y^3 = \frac{q^2}{k_t}x + C. {4}$$

Here it is used that q^2/k_t is independent of x. The integration constant C is determined from the boundary condition y(L)=H. After some manipulation we obtain

$$y(x) = \left(\frac{3q^2}{k_t}(x - L) + H^3\right)^{1/3}.$$
 (5)

Both q and k_t are unknown and they can be eliminated from equation (5) by extracting

$$\frac{q^2}{k_*} = \frac{y^3 - H^3}{3(x - L)} \tag{6}$$

and inserting the relation that holds at the seepage point, $y(x_0)=x_0/n$, to obtain

$$\frac{q^2}{k_t} = \frac{x_0^3 - n^3 H^3}{3n^3 (x_0 - L)}. (7)$$

By inserting (7) into (5) we obtain an expression for the phreatic surface without references to q or k_t

$$y(x) = \left(\frac{x_0^3 - n^3 H^3}{n^3} \frac{x - L}{x_0 - L} + H^3\right)^{1/3}.$$
 (8)

The seepage point x_0 is unknown. If the downstream side is "dry" or the downstream water stage is below the seepage outflow position, the location of seepage point x_0 can be determined either as in section 2.2; from the assumption that the phreatic surface is aligned with the downstream slope at the seepage point, or as by Solvik (1966); from the assumption that the seepage point adjusts so that the discharge is maximal. At the maximum it holds that

$$\frac{dq}{dx_0} = 0, (9)$$

and hence that

$$\frac{d}{dx_0} \left(\frac{q^2}{k_t} \right) = 0, \tag{10}$$

since k_t is a material parameter independent of x_0 . Performing a differentiation of equation (7) gives

$$\frac{d}{dx_0} \left(\frac{q^2}{k_t} \right) = \frac{3x_0^2 3n^3 (x_0 - L) - (x_0^3 - n^3 H^3) 3n^3}{\left(3n^3 (x_0 - L) \right)^2},\tag{11}$$

which is zero when the numerator is, i.e. when

$$3x_0^2(x_0 - L) - (x_0^3 - n^3 H^3) = 0. (12)$$

This equation can be transformed into the following form.

$$x_0^3 - \frac{3L}{2}x_0^2 + \frac{n^3H^3}{2} = 0. ag{13}$$

For a given dam geometry, x_0 is only a function of H. A review of Solvik's derivation reveals **a misprint or ambiguous definition of an angle parameter** that seems to have led to an erroneous utilization of his formulae. This answers probably the question why Solvik's analytical solution did not agree well with the experimental results.

Both q and k_t are important parameters when dealing with rock-fill dams. If one would like to determine one of them, the other has to be known. Their relation is given by equation (7).

When the above formulae are derived, assumptions are made that the seepage outflow point is located above the downstream level, denoted as h, or there is no water downstream. If the seepage point is submerged, i.e. $h > y_0$, the formula for the phreatic surface inside the dam is given by (Yang and Lovoll 2006)

$$y(x) = H \left(1 - \frac{1 - (h/H)^3}{L - nh} (L - x) \right)^{1/3}$$
 (14)

where h is the downstream level. The corresponding formula for the discharge is

$$q = \sqrt{\frac{k_t(H^3 - h^3)}{3(L - nh)}} \,. \tag{15}$$

Given a embankment dam geometry, the seepage discharge, as determined by equations (7) and (15), is a function of both the reservoir water depth H and the turbulent permeability k_t . It can be stated from equation (8) and (14) that the location of the phreatic surface, including the seepage outflow point, is only dependent on H and independent of k_t . If this is due to the assumption that the seeping flow takes place basically in the horizontal direction can be verified in the CFD modelling to be made below.

2.2 Seepage point location

The derivation of the cubic equation (13) for the seepage point can be done in different ways.

One way to go is to assume that the seepage point adjusts so that the discharge is maximal, i.e. by utilizing $dq/dx_0=0$, where again x_0 is the location of the seepage point, not the space coordinate in the horizontal direction. The latter statement is important since the same symbol, x, is used by Solvik to denote both the seepage point and the space coordinate.

Another way to derive equation (13) is to assume that the slope of the phreatic surface is parallel to the downstream slope at the seepage point. The fact that both ways result in the same equation implies that the assumptions are equivalent.

The following shows that the location of the seepage point x_0 , and hence the height of the phreatic surface y(x), can be derived from the assumption that the phreatic surface is aligned to the downstream slope at the seepage point, i.e. that

$$y'(x_0) = 1/n$$
. (16)

The result is equation (13), i.e. a cubic equation in x_0 that is identical to the one obtained by using the assumption by Solvik. Note that y' = dy/dx = I.

One possibility would be to differentiate equation (8) with respect to x and then insert equation (16), but the analysis is simplified if one instead considers

$$\frac{d}{dx}y^3 = 3y^2y' = \frac{3q^2}{k_t}. (17)$$

The last equality is motivated by equation (3). The rightmost part of equation (17) can be replaced using equation (7). By also using $y(x_0)=x_0/n$ we obtain the expression

$$y'(x_0) = \left(\frac{n}{x_0^2}\right)^2 \frac{x_0^3 - n^3 H^3}{3n^3 (x_0 - L)}$$
 (18)

Comparing equations (16) and (18), eliminating $y'(x_0)$, and multiplying by n give

$$1 = \frac{n^3 (x_0^3 - n^3 H^3)}{3n^3 x_0^2 (x_0 - L)},$$
(19)

which is satisfied if the denominator equals the numerator, i.e. if

$$x_0^3 - n^3 H^3 = 3x_0^2 (x_0 - L). (20)$$

Collecting terms yields obviously equation (13), i.e. the cubic equation in x_0 determining the location of the seepage point in the downstream slope.

The cubic equation corresponding to equation (13) is solved approximately by Solvik. However, *an explicit formula is available*! The physically relevant solution to equation (13) is

$$x_0 = L\left(\cos\left(\frac{\theta + 4\pi}{3}\right) + \frac{1}{2}\right),\tag{21}$$

where

$$\theta = \arccos\left(1 - 2\frac{n^3 H^3}{L^3}\right),\tag{22}$$

The fact that this solution is the only solution to equation (13) or (20) is motivated as follows. Equation (13), can be shown to have three real solutions if and only if

$$\frac{n^3 H^3}{L^3} \le 1,\tag{23}$$

see e.g. reference Math world or Råde and Westergren (1990). In addition, the roots are distinct if equation (23) holds with strict inequality. It is easy to see that equation (23) is always satisfied since n=L/H holds in the limiting case where the dam has a triangular shape and the upstream level H reaches the crest. In all other physically possible settings, n is less than L/H, so without omitting any relevant cases we can assume that equation (13) has three distinct real roots.

These roots are

$$x_{0,k} = L\left(\cos\left(\frac{\theta + k2\pi}{3}\right) + \frac{1}{2}\right), \quad k = 0,1,2,$$
 (24)

where

$$\theta = \arccos\left(1 - 2\frac{n^3 H^3}{L^3}\right),\,$$

Since $0 < n^3 H^3/L^3 < 1$ we have $0 < \theta < \pi$, and $1/2 < \cos(\theta/3) < 1$. Hence, for k=0 we have

$$L < x_{0.0} < 3L/2, \tag{25}$$

which is a non-physical solution since the seepage point must be located to the left of the intersection between the upstream level and the dam. Similarly, for k=1, we have $-1 < \cos(\theta/3 + 2\pi/3) < -1/2$, implying the likewise non-physical

$$-L/2 < x_{0,1} < 0 (26)$$

The remaining solution is obtained for k=2. Its feasibility is checked by observing that $-1/2 < \cos(\theta/3 + 4\pi/3) < 1/2$, and hence that

$$0 < x_{0,2} < L. (27)$$

3 Experiments

Laboratory experiments in a flume were performed at Vattenfall Research & Development AB (Johansson 1993). A 1.9 m high model dam was built of gravel of size ranging from 20-70 mm. The crest of the dam was 0.25 m wide, the upstream and downstream slopes were built with n = 1.65. The discharge and downstream levels were varied and the upstream level and the phreatic pressure at a number of locations were measured. The flow rate varied from 60 to 80 l/s. Related data extracted from the study is found in Appendix 1. Table 2.1 contains a summary of the experimental data defining the tested cases.

Table 3.1: Measured and given data defining the experimental cases.

	case 1	case 2	case 3	case 4
<i>H</i> (m)	1.48	1.54	1.71	1.72
<i>L</i> (m)	4.058	3.959	3.6785	3.662
$q (\text{m}^2/\text{s})$	0.060	0.065	0.081	0.0825
$x_0(m)$	1.551	1.551	1.716	1.716

The Reynolds number corresponds to at least Re = 950 in the study, which is clearly in the region of fully developed turbulent flow in the porous medium (Bear 1972).

4 Numerical solutions, CFD

A commercial finite volume code, Fluent version 6.2, was used to generate numerical solutions corresponding to the four test cases for which we have experimental measurements. The numerical model is two-dimensional and utilizes the volume of fraction (VOF) model to determine the position of the phreatic surface. The boundary conditions prescribe the level of the water surface at the upstream slope of the dam and the gauge pressure on the outflow, i.e. the downstream slope. Also the crest of the dam is considered to be an outflow boundary. The foundation where the dam rests on is modeled as an impermeable boundary.

The porous medium in the dam is modelled by an additional loss term in the momentum equation. The loss term *S* is determined by the power law,

$$S = -C_0 |V|^{C_1}. (28)$$

The term is related directly to the pressure gradient. Comparing equations (28) and (2), we see that $C_1=2$ and that $C_0=\rho g/k_t$. The water density ρ and the gravitational acceleration g are present due to that the pressure in the momentum equation is expressed in Pa, whereas the hydraulic gradient is the derivative of the height in m. There are other possibilities to define the loss term modelling porosity in Fluent, but the power law is sufficient here since we are dealing with isotropic permeability and a fully developed turbulent flow.

Parameter values in the CFD setup are ρ =999.7 kg/m³, μ =0.001304 Ns/m² (dynamic viscosity of water), g=9.82 m/s². The second order upwind discretization is used for momentum and volume fraction equations. The pressure interpolation scheme is "Body force weighted" and the pressure-velocity coupling is PISO. All relaxation parameters were set to 0.1 to ensure convergence and the iterations were terminated when the reduction of the residuals reached a factor of 10^{-5} .

The numerical simulations are proceeded by a grid refinement study where it is found that a grid with 240 000 cells gives results very similar to a grid with 960 000 cells. A coarser grid, with 60 000 cells, also gives reasonable results. As the discharge and seepage point location differs by a few percent compared to the finest mesh, it is decided to use the intermediate one with 240 000 cells.

The grid refinement is performed using H=1.48 m and $k_t=0.01$, which gives q=0.0532 m²/s. Changing the turbulent permeability to $k_t=0.0127$ gives q=0.0601 m²/s, which is the value for k_t we use from here on. An interesting observation made when comparing the results from $k_t=0.01$ and $k_t=0.0127$ is that a parameter change giving an increase of the discharge by 13% only affects the location of the seepage point by 0.22%. This indicates that the fact that, given an reservoir water level, the position of the phreatic surface is independent of k_t , which holds not only in the analytical solution, but also in a two dimensional CFD model where there is no assumption that the velocity is horizontal.

Figure 4.1 shows the interface between the water phase and the air as computed by CFD for case 1. When using the VOF model, the concentration of water is computed as a continuous fraction of unity. The water surface is defined to be located where the fraction is 1/2 and it is desirable with a sharp interface. The interface in Figure 4.1 can be considered as sharp.

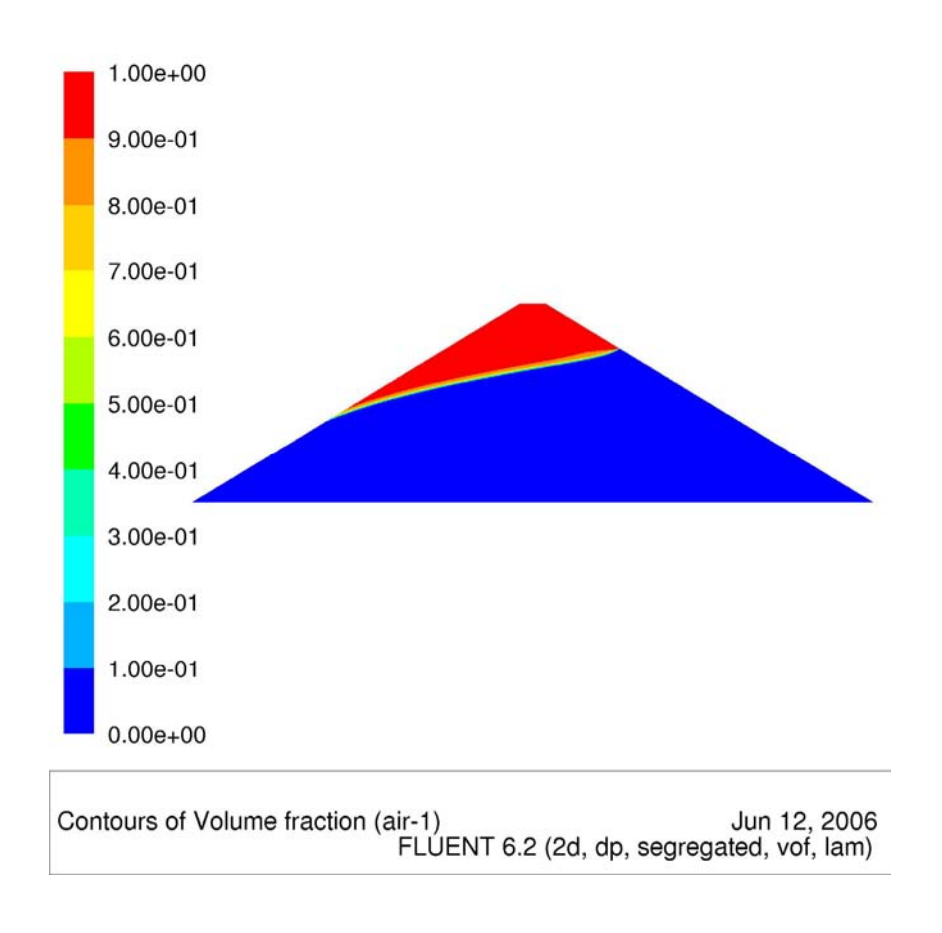


Figure 4.1: The interface between water (blue) and air (red) as computed by CFD.

Figure 4.2 shows the flow path lines for case 1. It is apparent that the flow velocity vector is not strictly horizontal. The assumption of only horizontal velocity component is made when the analytical solution is derived, as did by Solvik.

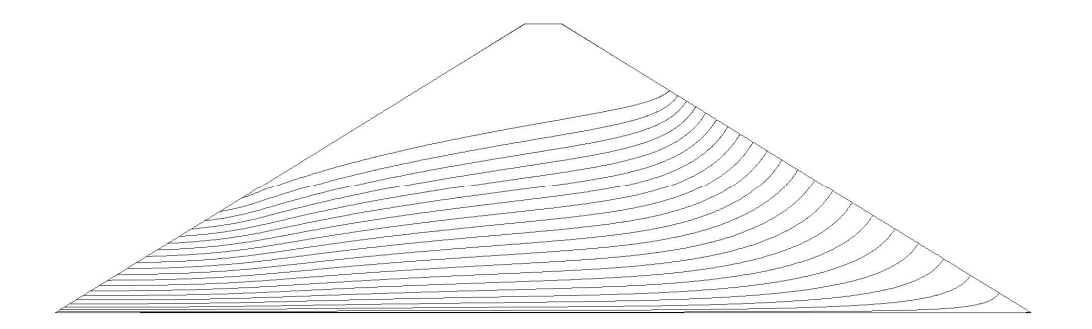


Figure 4.2: Path lines for the flow through the dam as computed by CFD

5 Results and comparisons

The four cases defined in Table 3.1 are used in order to compare both the analytical solution and the CFD computations to the experimental measurements.

5.1 Seepage point location

The first comparison concerns the location of the seepage point. This is independent of k_t in the analytical solution and at least rather independent in the CFD computations. The results are displayed in Table 5.1.

Table 5.1:	Comparison of seepag	e point locations.
-------------------	----------------------	--------------------

<i>x</i> ₀ (m)	case 1	case 2	case 3	case 4
experiment	1.551	1.551	1.716	1.716
Analytical	1.224	1.335	1.720	1.747
CFD	1.333	1.446	1.806	1.832

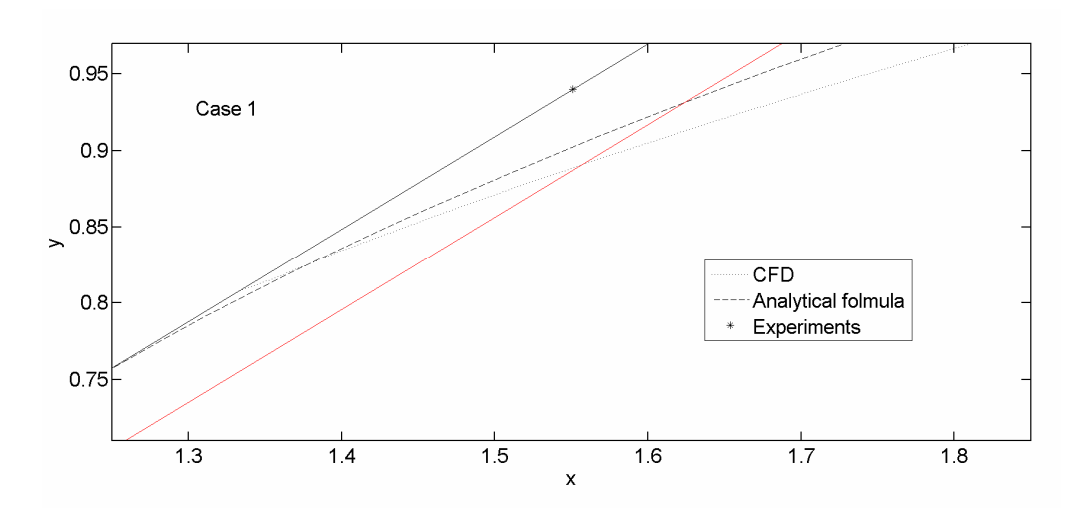


Figure 5.1: Seepage outflow position in downstream slope, case 1. The red line is an artificial inner surface at a distance of 70 mm from the real slope.

One feature of the phreatic surface is that it is aligned with the downstream slope at the seepage point. This implies that small defects in the surface at some distance above that level might intersect the water surface, yielding a considerable disturbance of the measured seepage point. An elementary investigation was performed by introducing an inner downstream slope at a distance of 70 mm from the real slope, see Figure 5.1 where the red line is the artificial inner slope. The distance was chosen as the largest diameter of the gravel used in the experiments. It can be seen that the phreatic surface computed by CFD intersects that inner slope at about x = 1.56 for case 1. The corresponding value for the surface computed according to Solvik is x = 1.62.

5.2 Seepage discharge

Both the analytical solution and CFD demands good knowledge of the turbulent permeability k_t in order to present reasonable values regarding the discharge q. If, as in the available experimental cases, one knows both the location of the seepage point and the discharge, it is possible to compute the turbulent permeability using equation (7). This is however not completely satisfactory, since the measured seepage point is likely to differ from the one computed analytically using equation (21). An approach that is more mathematically stringent is to compute k_t from the measured q and the computed x_0 . Both versions are given in Table 5.2.

In Table 5.2, it shows that the variation is small, especially for cases 3 and 4. One possible explanation for that the difference is smaller for these cases is that the flow is more turbulent as the discharge and velocity are larger. These cases are hence better described by the theory.

Table 5.2: Turbulent permeability from the analytical solution

	case 1	case 2	case 3	case 4
k_t from measured q and measured x_0	0.0112	0.0108	0.00997	0.0100
k_t from measured q and computed x_0	0.0108	0.0107	0.00997	0.0100

In the following, we consider case 1 as a calibration case and use $k_t = 0.0108$ with the analytical solution. In the CFD computations we use $k_t = 0.0127$, cf. section 4. Table 5.3 shows the resulting discharges.

Table 5.3: Comparison of seepage discharges

q	case 1	case 2	case 3	case 4
experiment	0.060	0.065	0.081	0.0825
analytical, $k_t = 0.0108$	0.060	0.0655	0.0843	0.0856
CFD, $k_t = 0.0127$	0.0601	0.0656	0.0821	0.0827

5.3 Phreatic surface

Figures 5.2 to 5.5 show comparisons of the phreatic surfaces computed by CFD and the analytical solution, together with experimental measurements. An important difference between the analytical solution and CFD can be observed at the upstream slope, where the angle between the slope and the phreatic surface differs substantially.

Note the double measurements at x=2.0 m and x=3.5 m. The larger values are from measurements performed at locations closer to the surface.

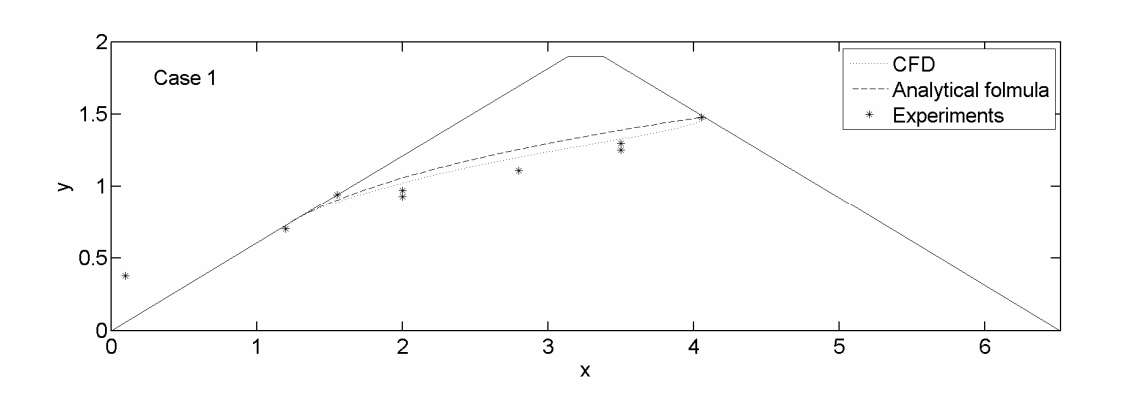


Figure 5.2: Phreatic surfaces and measurements for case 1.

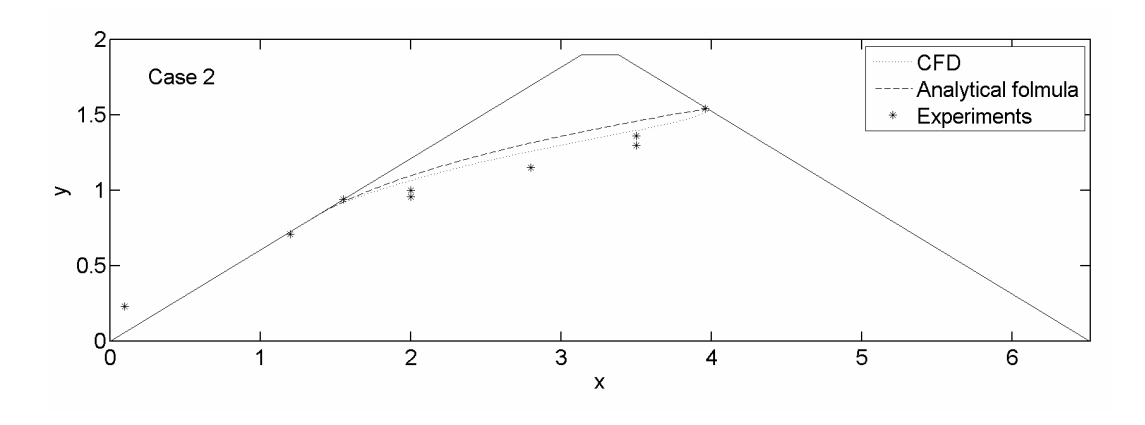


Figure 5.3: Phreatic surfaces and measurements for case 2.

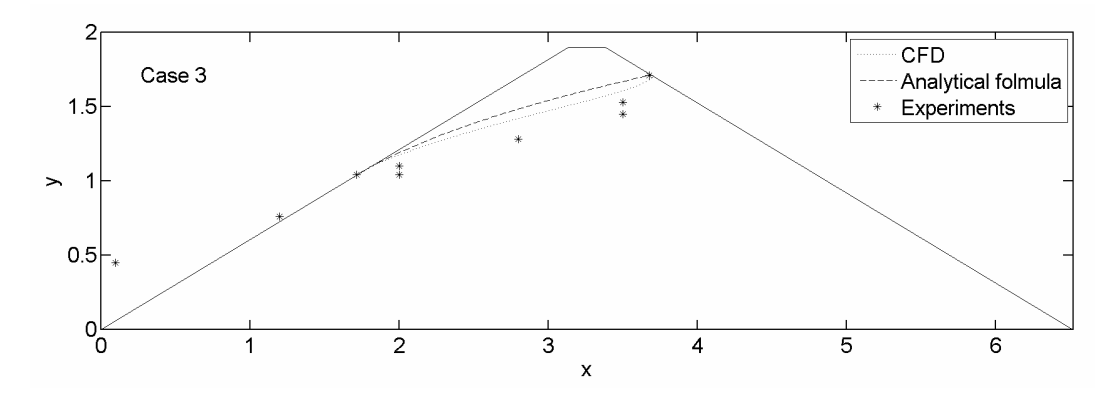


Figure 5.4: Phreatic surfaces and measurements for case 3.

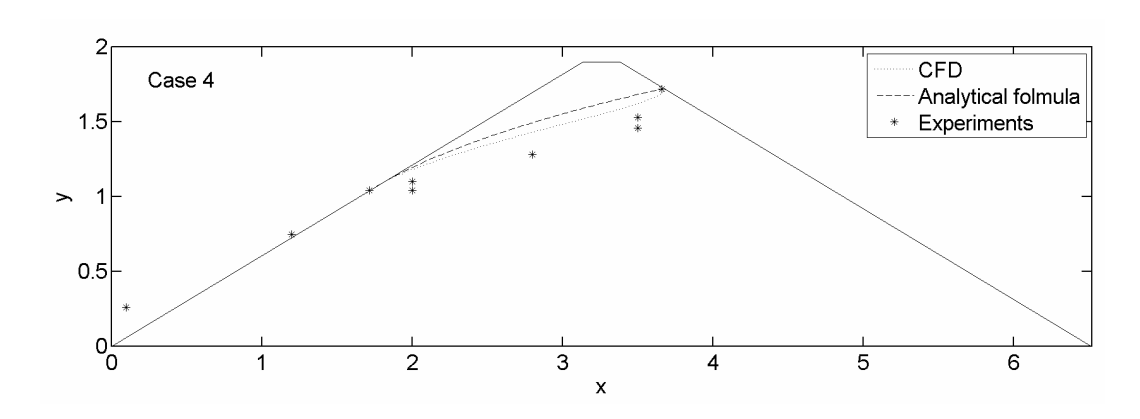


Figure 5.5: Phreatic surfaces and measurements for case 4.

6 Conclusions

The agreement between the analytical solution, CFD modelling and experimental measurements are good, especially concerning the seepage point location. When judging the differences, one must bear in mind that the situation at the downstream slope is idealized and considered to be straight and homogeneous in the computations. In the experiments, the size of the gravels is considerable compared to the differences in the results.

Both CFD and the analytical solution differ from the measurements in the phreatic surface inside the dam. The difference is somewhat smaller for CFD, about half of the difference between the analytical solution and the experiments. A possible reason is that the vertical velocity is considered in the CFD model.

Calibration is made to determine which value to use of the turbulent permeability. A value that yields good agreement with the discharge is used. This procedure yields different values for CFD and the analytical solution. One explanation is that the calibration accounts for the imperfections of the theoretical models. These imperfections are of different nature in CFD as compared to the analytical solution.

The study shows that if a case of one discharge is used for calibration, CFD is better than the analytical solution in determining the discharge for other cases.

Both CFD and the analytical solution overestimates the height of the phreatic surface inside the dam. This situation could be explained by systematic errors in the method used to measure the surface in the experiments. An argument for this is that when double measurements are available, it is the sensor closest to the surface that yields the higher value and hence a better agreement with the computations.

The final comment is that the analytical solution is somewhat less accurate but much easier to use than the CFD modelling.

References

- [1] J. Bear, Dynamics of fluids in porous media, Elsevier 1972.
- [2] N. Johansson, Fyllningsdammar, genomströmning och stabilitet av nedströmsslänt. In Swedish. Vattenfall Utveckling AB, rapport VH-H 93:B8, 1993.
- [3] Math world, web page http://mathworld.wolfram.com/CubicFormula.html.
- [4] L. Råde and B. Westergren, BETA Mathematics Handbook, 2nd ed., Studentlitteratur 1990.
- [5] O. Solvik, To-dimensional turbulent stromning gjennom isotrop steinfylling. In Norwegian. Norges tekniske hogskole, Trondheim, Vassdrags- og havnelaboratoriet. Meddelelse 8N 1966.
- [6] J. Yang and A. Lovoll, Turbulent seepage in a 6-m rock-fill dam field measurements, analytical and numerical solutions, ICOLD Congress, Barcelona 2006.

Appendix A: Experimental data

The dam used in the experiments is depicted in Figure A.1. The drawing is taken from the study by Johansson (1993). The direction of the flow is from left to right in Figure A.1, which is the opposite compared to Figure 2.1. The phreatic surface was measured in the points denoted by numbers. Here we use all points but no. 52 and 54, as those are located at a separate plane through the dam. The measurements as reported are displayed in Table A.1. Figure A.2 shows the dam from the downstream side. The net is used to stabilize the slope.

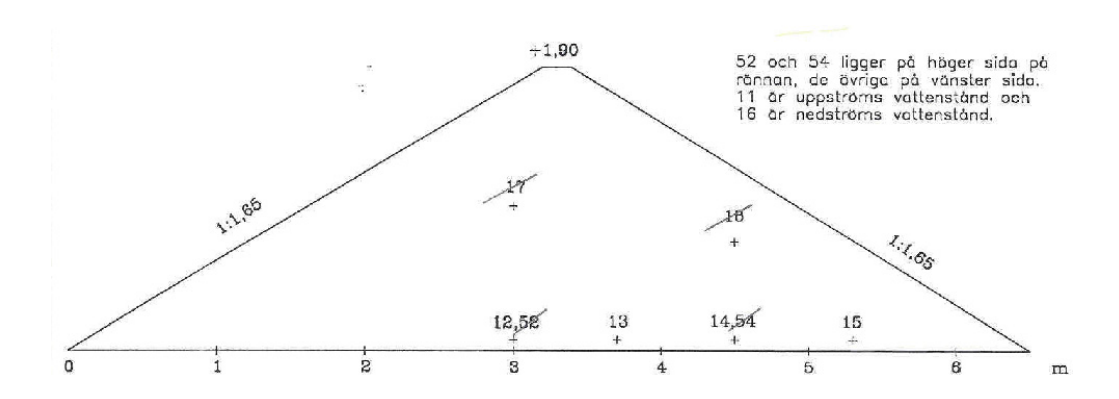
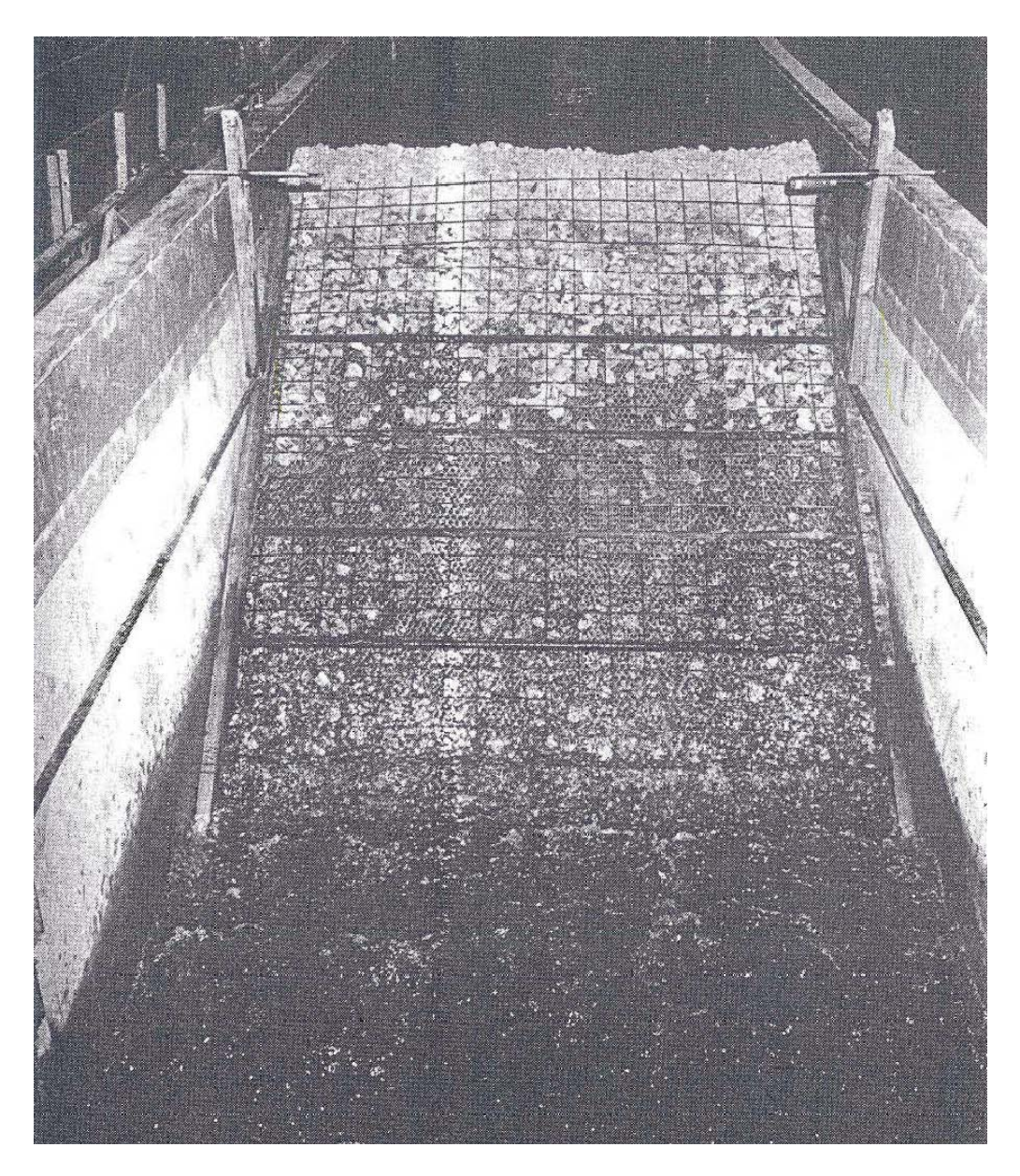


Figure A.1 Geometry of experimental dam and measurement locations of phreatic surface

Table A.1 Measurements as reported by Johansson (1993).

	FLÖDE L/S-M			
Tryckuttag	60	65	81	82,5
11	1,48	1,54	1,71	1,72
12	1,25	1,30	1,45	1,46
52	1,24	1,29	1,45	1,46
13	1,11	1,15	1,28	1,28
14	0,93	0,96	1,04	1,04
54	0,93	0,95	1,04	1,04
15	0,70	0,71	0,76	0,75
16	0,38	0,23	0,45	0,26
17	1,30	1,36	1,53	1,53
18	0,97	1,00	1,10	1,10
Källsprång	0,94	0,94	1,04	1,04



 $\label{eq:Figure A.2} \textbf{ The dam used in the experiments as seen from downstream.}$



ELFORSK

SVENSKA ELFÖRETAGENS FORSKNINGS- OCH UTVECKLINGS – ELFORSK – AB Elforsk AB, 101 53 Stockholm. Besöksadress: Olof Palmes Gata 31 Telefon: 08-677 2530. Telefax 08-677 2535 www.elforsk.se